4

Raman Spectroscopy: A Non-Destructive and On-Site Tool for Control of Food Quality?

S. Hassing[1], K.D. Jernshøj[2] and L.S. Christensen[3]
[1]*Faculty of Engineering, Institute of Technology and Innovation, University of Southern Denmark,*
[2]*Faculty of Science, Department of Biochemistry and Molecular Biology, Celcom, University of Southern Denmark,*
[3]*Kaleido Technology, Denmark*

1. Introduction

In recent years there has been an increasing focus from the consumers on food quality i.e. unwanted substances such as bacteria, pesticides, drug residues and additives as well as on food composition including nutritional value, healthy additives, antioxidants and the contents of selected fatty acids. This is also reflected in an increasing interest for organic food products. It therefore seems appropriate to develop substance specific, non-destructive and fast measuring techniques that can be used close to the consumer, for monitoring different properties of food products.

Raman spectroscopy is an example of a fast, non-destructive and molecule specific technique. As discussed in section 2, Raman spectroscopy involves illuminating the sample with laser radiation with wavelengths either in the near-infrared (NIR), visible or ultraviolet (UV) regions, monitoring the light reflected from the sample and analyzing the intensities as a function of wavelength.

The focus of the chapter is to discuss the applicability of Raman spectroscopy as a non-destructive and molecule specific tool for monitoring food quality. This goal is achieved through a discussion of the basic properties of Raman scattering (RS) and experimental aspects, followed by a discussion of three case studies: 1. Revelation of a pork content in minced lamb products, 2. Detection and classification of nearly identical anti-oxidants and 3. Detection of pesticides on fruits and vegetables using surface enhanced Raman scattering (SERS).

In general the requirements to any experimental method suitable for an on-site evaluation of food quality are:

1. robust and easy to use instrumentation
2. portable instrument
3. non-destructive measurements
4. no or a minimum of sample preparation
5. a fast acquisition time
6. a qualitative and quantitative determination of chemical constituents
7. a high molecular specificity
8. a measurement of low concentrations of unwanted contents

Several of these requirements can be met by optical techniques based on some kind of reflection measurement. The importance of the different requirements will depend on the specific application, e.g. are the development and implementation of the technique highly dependant on, whether the commodity should be controlled for an unwanted or wanted content. Both types of content place requirements on the molecular specificity, however, in the case of detecting an unwanted content, the concentration is often very low as well.

Figure 1 illustrates the contents of information obtained from three different kinds of reflection measurements performed on the same green leaf.

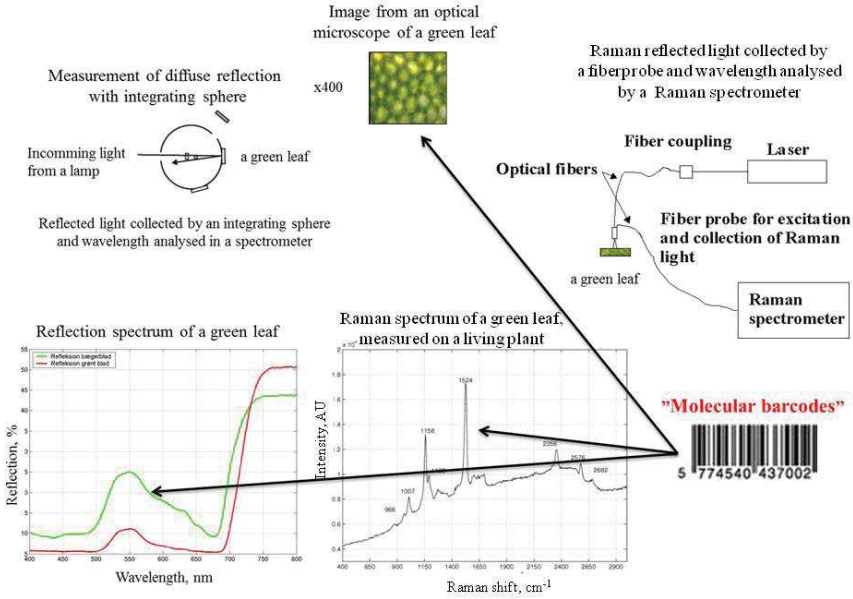

Fig. 1. Optical reflections with different information content from a green leaf. Left: Diffuse reflection (multiple scattering), middle: Diffuse reflection and imaging and no quantification of the spectral information is made, except the information visible to the human eye. To the left is shown a diffuse reflection spectrum of the same leaf (red curve) obtained with a Perkin Elmer, λ900 spectrophotometer equipped with an integrating sphere. The integrating sphere collects all the light reflected from the leaf enabling an absolute measurement of the reflectance coefficient. Reflection measurements performed on different kind of green plants and on different plant parts are similar and contain almost identical spectral information. The example in figure 1 shows reflection spectra from two types of leaves of a Hibiscus, rosa sinensis, namely a foliage leaf and a sepal Jernshøj & Hassing (2009). The spectra shows differences in the absolute reflection values, but are very similar with respect to spectral

information. The similarity is partly due to a blurring of the molecular signal caused by the molecular interaction with the surroundings and partly, since the molecular signal in itself is a composite signal reflecting both the motions of the electrons and nuclei in the molecule. A closer study shows a higher concentration of secondary pigments, e.g. carotenes, in the sepals than in the green leaves. A quantitative analysis of chlorophyll and carotenoid from these spectra is possible, when applying empirical models, this reflects the complex scattering and interaction processes taking place in the leaf Jernshøj & Hassing (2009); Kortüm (1969). However, due to the poorly resolved spectra, it may be impossible to discriminate between the presence of closely related molecular species, such as the antioxidants α- and β-carotene.

The right part of figure 1 shows a Raman spectrum obtained from the same foliage leaf. As opposed to the diffuse reflection measurements, the application of a laser results in the generation of a molecular reflection signal with measurable intensity, namely the Raman scattered light. As clearly seen from the figure, the spectral information is increased dramatically in the Raman spectrum. As discussed in the next section, the spectral distribution observed in the spectrum primarily reflects the vibrational motion of the nuclei in the "naked" molecules.

Summarizing: The outcome of an optical reflection measurement may be compared to a bar code, which is a well known component in different industries, where different and often high information content is encoded into this code and placed on a commodity. The information is read out by measuring the reflected laser light from the bar code, an example being the price scanner used in supermarkets. The difference between this bar code and the molecular information, is that the "molecular bar codes" are native parts of the sample, which are basically determined by the molecular composition. The informational quality of the particular "molecular bar code" obtainable is defined by the type of interrogative process used, e.g. imaging, diffuse reflection or Raman scattering.

2. Raman spectroscopy

The section gives an introduction to Raman scattering and point to the potential inherently present in the Raman effect with respect to obtain detailed molecular information. The section focuses on the theoretical and experimental challenges that have to be overcome in order to make different kinds of Raman techniques valuable diagnostic tools in the analysis of food quality.

Raman spectroscopy involves illuminating the sample with laser radiation with wavelengths either in the NIR, visible or UV regions, which excites the constituent molecules within the sample to vibrate. A vibrational Raman spectrum of the molecules is obtained by collecting the in-elastically scattered light. Each molecule present in the sample has a characteristic set of nuclear vibrations and thus the sample as a whole has a unique vibrational signature, i.e. a "molecular bar code" with a high information content. Raman spectroscopy is a class of well-documented, non-destructive, optical techniques with a high spectral resolution all of which are based on the Raman effect discovered by C. V. Raman in 1928 Raman & Krishnan (1928). Today more than 25 different Raman spectroscopies are known Long (2002).

2.1 An experimental view on Raman spectroscopy

Raman spectra can be obtained as reflectance measurements, which means that samples can be investigated with no or very little sample preparation and as opposed to other widely

applied optical techniques, such as NIR and Fourier Transformed Infrared (FT-IR), Raman measurements are not influenced by the presence of water and therefore biological samples can be measured in their natural environment. Besides, the samples are not influenced by the measurements and the same samples can be investigated over time, which is essential, when measuring on food samples. Since the spectral information contained in a non-resonance Raman spectrum (vide infra) is virtually independent of the laser wavelength and since a complete Raman spectrum, typically 0 - 3500 cm^{-1}, only covers a wavelength region of approximately 100 nm (the exact value depends on the specific laser wavelength), it follows that complete Raman spectra of food products can be measured without removing the protective film covering the products, just by choosing a laser wavelength that matches the optical window of the protective film.

Raman spectrometers may be divided into two classes: Dispersive instruments and FT-Raman instruments. Any dispersive Raman spectrometer consists essentially of four components, a filter to block the Rayleigh scattered light, an entrance slit (often defined by an optical fiber), a transmission or reflection grating, where in the latter case the focusing optics is built into the grating and a CCD detector, which is coupled to a computer. The image of the illuminated entrance slit or fibre core is formed on the CCD and the different wavelengths contained in the Raman signal is converted by the grating into different positions on the CCD. Because of the simplicity of the basic Raman spectrometer, it is possible to build different editions for different purposes.

Figure 2a shows a typical Raman spectrometer, suited for scientific purposes. The setup, which is developed at The Molecular Sensing Engineering group, Faculty of Engineering, Institute of Technology and Innovation, University of Southern Denmark, has been built having a high degree of flexibility in mind. This flexibility allows us to arrange and rearrange the setup according to the experimental conditions necessary to achieve the desired molecular information. One of the main research areas is molecular investigations on bio-molecules, such as porphyrin and haemoglobin doing resonance and non-resonance Raman spectroscopy, polarized and unpolarized experiments as well as Surface Enhanced Resonance Raman Scattering (SE(R)RS) Jernshøj & Hassing (2010). Especially research involving polarized Raman measurements, where the molecular information obtained using linearly or circularly polarized light, has been carried out on a number of different samples. Recently, the molecular information obtained from such polarized measurements on a highly symmetric gold nanostructure (SE(R)RS) has been investigated in details K. D. Jernshøj & Krohne-Nielsen (2011).

When combining a Raman spectrometer with an optical microscope, the information content may be further increased. The Raman setup in figure 2a consists of a modified Olympus BX60F5 microscope, a SpectraPro 2500i spectrograph from Acton (Gratings: 1200 and 600 lines/mm) and a cooled CCD detector from Princeton Instruments, model Acton PIXIS. The setup is equipped with 12 different laser excitation wavelength, provided by: a 532 nm diode laser (Ventus LP 532), a Spectra Physics 632.8 nm HeNe laser, a Spectra Physics Ar^{+} laser: visible region and a tunable Ti3+:sapphire (titanium sapphire) laser: visible and NIR region. The setup has adjustable spectral, $5cm^{-1}$ and spatial resolutions, 0.3μm. Since the Raman spectrometer is combined with an optical microscope, equipped with a motorized, translational XY-stage (Thorlabs Inc., CRM 1) on the microscope translational stage, it is possible to obtain complete Raman spectra from different points across the sample. Due to the high spatial resolution (0.3μm) it is possible to perform Raman Imaging with a subcellular

Fig. 2. The Raman equipment at The Molecular Sensing Engineering group at Faculty of Engineering, Institute of Technology and Innovation, University of Southern Denmark. (a.) The Raman setup, which is suited for scientific purposes. The Raman spectrometer is combined with an optical microscope, which is equipped with a motorized XY-stage on the translational stage. (b.) A portable commercial Raman setup: DeltaNu Inspector Raman, 785 nm excitation, unpolarized Raman, spectral resolution: 10, 12 or 15 cm^{-1}, predefined laser power 1.8, 3.4 and 6 mW, polystyrene standard for wavelength calibration, battery operated. Inspector Raman has been equipped with a manual translational XY-stage, order to be able to translate the laser across the sample.

spatial resolution, which has proven especially useful combined with multivariate analysis in the study related to early diagnosis of human breast cancer cells Martin Hedegaard & Popp (2010). As discussed in case study 3.1, Raman imaging combined with a machine vision system can be applied in an automatized determination of the composition of inhomogeneous food products, such as minced meat products.

For the purpose of an on-site, non-destructive investigation, the laboratory is also equipped with a commercial portable Raman spectrometer, which is shown in figure 2b. The parameters of this turn-key instrument are: 785 nm excitation, unpolarized Raman measurements, predefined spectral resolutions: 10, 12 or 15 cm^{-1}, predefined laser power 1.8, 3.4 and 6 mW, polystyrene standard for wavelength calibration and finally the possibility for battery operation. According to requirement 2 on page 2, dealing with portability, this kind of small Raman spectrometer is suited for field use, since it may be battery operated and is portable. Besides, the spectrometer has been equipped with a manual XY-stage in order to be able to scan the laser across the samples, when measurements are done on inhomogeneous samples.

As will be discussed in the next section, laser induced fluorescence, which is excited simultaneously with the Raman process, may often be a serious problem in practical applications of Raman spectroscopy. The fluorescence can be avoided in most cases by choosing the laser wavelength in the NIR region. When this choice is combined with an instrument that has a high sensitivity (high through-put), Raman spectra of high quality can be obtained. In FT-Raman spectrometers the grating is replaced by a scanning interferometer (e.g a Michelson interferometer) by which an interferogram, i.e. a time signal containing the spectral distribution of the Raman signal, is measured. The Raman signal is calculated by a computer by performing a fast Fourier transform of the interferogram data. A FT-Raman

spectrometer consists of the following components: a NIR-laser with wavelength 1064 nm, filters to block the Rayleigh scattered light, a stable and efficient interferometer, a sensitive detector coupled to a computer, which includes software with the capability of performing fast Fourier transform. Typically, FT spectrometers are scientific instruments but it is possible to buy a FT-Raman spectrometer, e.g. RamanPro, which is designed to measure chemicals in production environments (http://www.rta.biz/).

Since different portable, commercial Raman instruments with different specifications are available, it will be possible to optimize the application with respect to the specific goal by applying e.g. either multivariate analysis, some form of enhancement of the Raman signal and specially developed additional software. Notice, that in the case of FT-Raman instruments the above mentioned flexibility with respect to choosing the laser wavelength is limited.

2.2 Fragments of Raman theory

As mentioned previously Raman spectroscopy involves illumination of the sample with laser radiation with wavelengths either in the NIR, visible or UV regions. According to quantum mechanics the intensity of a laser beam is proportional to the number of photons and the photon energy Long (1969). In molecular spectroscopy it is custom to measure the molecular and photon energy in the unit cm^{-1}, where x $cm^{-1} = 10^7/y$ nm. This means that the photon energy of a NIR laser with wavelength y = 785 nm is equal to x = 12739 cm^{-1}, while the photon energy for a visible laser with wavelength 532 nm is 18797 cm^{-1}. Thus, the photon energy is inversely proportional to the wavelength.

When the wavelength of the laser is chosen in the spectral region, where the molecules in the sample do not absorb any light, a fraction of the laser light is scattered. Most of the scattered light will deviate from the incident laser light only in the direction of propagation, but will have the same wavelength as the laser. This scattering process is known as Rayleigh scattering. A small fraction of the scattered light, namely the Raman scattered light, will in the scattering process also be shifted in wavelength. These measurable shifts are determined by the physical properties of the scattering molecule and they appear in the Raman spectrum as characteristic sharply defined peaks as seen in figure 1. Since each molecule gives rise to a characteristic and unique Raman spectrum, we are presented with a "molecular bar code" with a high information content. In vibrational Raman spectroscopy, the spectra reflect that each molecule has a characteristic set of nuclear vibrations. Besides, being shifted in wavelength the polarization of the Raman scattered light may also be different from the polarization of the laser light. The shift in polarization is determined by the nature of the various nuclear vibrational motions, which are also determined by the molecular properties. The quality of the information contained in the "molecular bar code" can therefore be increased by including the shift in polarization in the analysis.

In the following we focus on some of the basic principles describing the Raman process, which are necessary to illustrate the potential of and difficulties with Raman spectroscopy, when applied in food analysis. The fundamental theory, various aspects and applications of Raman scattering have been extensively discussed in the literature and we refer to these for further details eds. R. J. H. Clarke & Hester (n.d.); Long (2002); McCreery (2000); Mortensen & Hassing (1980); Plazek (1934); Smith & Dent (2005).

Figure 3 gives a schematic overview of the Raman process (left) and the fluorescence process (right) and the basic expression for the Raman intensity I_{Raman} is given in Eq.(1).

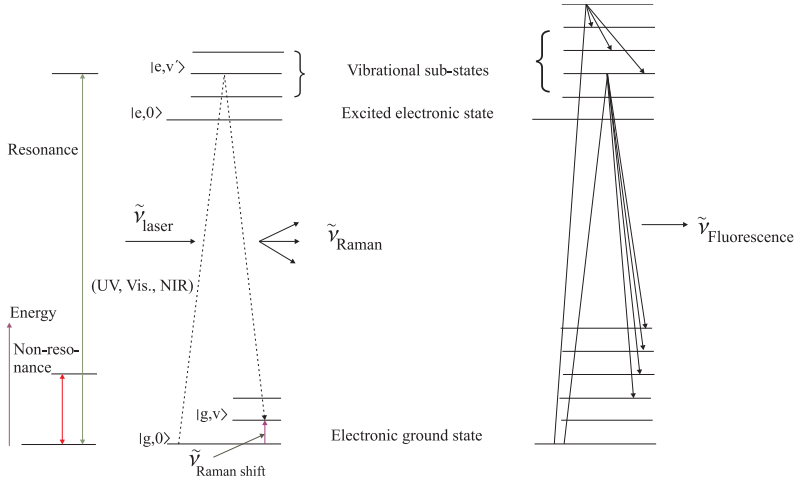

Fig. 3. Left: The Raman process is a *coherent* absorption-emission sequence. Right: Fluorescence is a real absorption followed by a spontaneous emission process, i.e. an *incoherent* absorption-emission sequence.

$$I_{Raman} \propto \tilde{\nu}_{Raman}^4 \left| \sum_{e,v'} \frac{\langle gv|\rho|ev'\rangle\langle ev'|\sigma|g0\rangle}{\tilde{\nu}_{ev',g0} - \tilde{\nu}_{laser} - i\gamma_{e,v'}} + \frac{\langle gv|\sigma|ev'\rangle\langle ev'|\rho|g0\rangle}{\tilde{\nu}_{ev',gv} + \tilde{\nu}_{laser} + i\gamma_{e,v'}} \right|^2 \cdot I_{laser} \tag{1}$$

The horizontal bars represent the energy of the molecular states, 0 is the vibrational ground state (indicating that none of the molecular vibrations are excited) and v is the final vibrational state. $|g,0\rangle$ and $|g,v\rangle$ are the symbols for the initial and final molecular states participating in the Raman process, where g denotes the electronic ground state and 0 and v the vibrational substates of the initial and final states. $|e,v'\rangle$ denotes an electronic excited state in the molecule and its vibrational substate. $\rho,\sigma = x,y,z$, where $e\cdot\rho$ is the electric dipole moment (e is the charge of an electron). Since each molecule has a characteristic set of nuclear vibrations, v and v' are really sets of numbers, where the value of each number describes the degree of excitation of each kind of vibrational motion. Thus, $v = v_1, v_2, ...v_k, ...v_{3N-6}$, where N is the number of nuclei in the molecule. In the benzene molecule e.g., where $N = 12$, the set will consist of thirty numbers, corresponding to the thirty different kind of vibrations that may be excited.

The Raman process can be thought of as a *coherent* absorption - emission sequence, in which the absorption of the incoming laser light is followed by an immediate re-emission of the Raman scattered light. During the initial absorption the molecule shifts state from $|g,0\rangle$ to $|e,v'\rangle$, while during the re-emission the molecule shifts state from $|e,v'\rangle$ to $|g,v\rangle$. In non-resonance Raman Scattering, where the photon energy of the laser (illustrated by the red arrow in figure 3) is small compared to the energy of any electronically excited state, all molecular states, $|e,v'\rangle$, contribute to the scattering process and thereby to the intensity of a particular Raman line in the spectrum. This is reflected through the appearance of a summation over all molecular states of the molecule in the theoretical expression for the Raman scattered intensity given in Eq.(1).

For comparison, the fluorescence process is illustrated to the right in figure 3. This process is an *incoherent* absorption - emission sequence, which consists of a genuine absorption of incident light followed by a genuine emission of light. As illustrated in the figure, the initially excited molecule is allowed to shift state before it spontaneously emits light, which destroys the coherent nature of the sequence. When focussing on the emission spectrum (i.e. the fluorescence), the molecule may during the emission end up in different vibrational substates. Since the contributions from all the possible transitions have to be added together in the expression for the emission intensity and since the number of vibrational motions, $3N-6$, may be very large for molecules typically appearing in food products, the different contributions to the intensity overlap with the result that the spectral distribution in the fluorescence spectra becomes broad and without much structure. This decreases the quality of the "molecular bar code" related to fluorescence. Depending on the experimental conditions, both the Raman and fluorescence processes may be initiated simultaneously. This is illustrated in the Raman spectrum of the green leaf in figure 1, where the Raman spectrum "rides" on top of a broad fluorescence background. The fluorescence may even be so pronounced that the Raman spectrum is partly or completely hidden. One way to avoid the excitation of fluorescence is to choose a laser with a photon energy smaller than any electronic excitation energy of the molecules.

It follows from the expression for the Raman intensity given in Eq.(1) that the intensity is proportional to the intensity of the laser and proportional to the fourth power of the photon energy of the Raman scattered light. The energy of the final molecular state termed $\tilde{\nu}_{Raman\ shift}$ is equal to $\tilde{\nu}_{Raman\ shift} = \tilde{\nu}_{laser} - \tilde{\nu}_{Raman}$. In Raman spectroscopy one measures I_{Raman} as a function of $\tilde{\nu}_{Raman\ shift}$, see figure 1. Since $\tilde{\nu}_{Raman\ shift}$ is equal to a vibrational energy of the molecule, the Raman spectrum depicts the characteristic vibrations of the molecule. Vibrational energies are typically much smaller than the excited electronic energies of a molecule, this means that the Raman intensity is approximately proportional to the fourth power of the photon energy of the laser. Experience shows that the fluorescence may in most cases be avoided by choosing a NIR laser with wavelength 1064 nm, which corresponds to the photon energy: 9399 cm^{-1}. Comparing the latter with the photon energy of the visible laser with wavelength 532 nm, the Raman intensity is reduced by a factor 16. The loss of Raman intensity is in the FT-Raman spectrometers mainly compensated for by the removal of fluorescence combined with the high sensitivity that can be obtained in these instruments Vidi (2003).

The central part of the expression is the absolute square of the molecular polarizability, $\boldsymbol{\alpha}_{\rho\sigma}$, where $\boldsymbol{\alpha}_{\rho\sigma}$ describes the change in the electron distribution of the molecule in response to the interaction with the incoming laser light. Each numerator in $\boldsymbol{\alpha}_{\rho\sigma}$ contains a product of two terms, where each term is called the transition dipole moment, reflecting the transitions taking place in the molecule during the scattering process. The magnitude and sign of these in combination with the magnitude and sign of the denominator determine the contribution from a specific molecular state to the intensity of a particular Raman line. The appearance of the absolute square of the sum of these contributions reflects the coherent nature of the Raman process. In fluorescence both the absorption and the re-emission processes are independent and determined by the absolute square of each transition moment. *In fact, the higher information content observed in Raman spectroscopy has origin in the coherent nature of the Raman process*. The real part of the denominator in the first term, called the resonance term, contains the energy difference between the energy of the excited state $|e,v'\rangle$ and the photon energy of

the laser, $\tilde{\nu}_{ev',g0} - \tilde{\nu}_{laser}$. The imaginary term reflects the energy broadening of the state $|e, v'\rangle$. If the photon energy of the laser is chosen equal to $\tilde{\nu}_{ev',g0}$, the contribution from this state to the Raman process becomes dominating causing the Raman signal to be enhanced. The enhancement depends on the value of the imaginary term but the enhancement may typically be of the order of magnitude 10^4 to 10^6. The phenomenon is termed Resonance Raman Scattering (RRS) and is illustrated with the green arrow in figure 3. In practice the molecular states close to the resonant state will give the largest contribution to Raman scattering. In RRS it is possible to get information about the participating excited states, whereas in non-resonance this information is smeared out.

A large bio-molecule, e.g. present in various food products, has a large number of characteristic vibrations. Although, not all of them are seen in the Raman spectra, the spectra may often be very complex, i.e. the "molecular bar code" contains a lot of information. Raman scattering can be performed in several ways with the result that specific parts of the obtainable molecular information may be reached, i.e. distinct parts of the "molecular bar code" is read out. Resonance enhancement of the Raman signal can be utilized to obtain information about specific parts of a large molecule, e.g. if the molecule contains a chromophore, it is possible to select the laser wavelength close to an electronic absorption of the chromophore with the result that only those vibrations involving the nuclei of the chromophore are enhanced and therefore seen in the Raman spectrum. A chromophore is the part of a molecule responsible for its color, where the color arises, when the molecule absorbs certain wavelengths of visible light and transmits or reflects others.

A special kind of resonance Raman spectroscopy, termed Raman Dispersion Spectroscopy (RADIS) Mortensen (1981), involves a quantitative comparison of Raman spectra measured with a few different excitation wavelengths close to the electronic resonance of the chromophore. The 3D graph in figure 4 shows the possibilities with RADIS. For each excitation wavelength the corresponding Raman intensity can be followed as a function of the Raman shift, while when choosing a specific Raman shift, the intensity of this can be followed as a function of the excitation wavelength. Due to the narrow line width of the Raman spectra and the coherent nature of the Raman process each Raman band has its own and distinct excitation spectrum (termed an excitation profile).

As discussed in subsection 3.2 this enables discrimination between molecularly almost identical constituents, such as α- and β-carotene even when the amount of one of the constituent is very small compared to the other.

2.3 Improving Raman sensitivity by nanotechnology

Raman spectroscopy has two serious limitations: First, Raman scattering is inherently a weak effect (typically 10^8 incoming laser photons only generate 1 Raman photon) and secondly, fluorescence is often emitted concurrently with the Raman scattering. Since the fluorescence signal is typically 4 to 8 orders magnitude larger than the Raman signal, this will be hidden in the fluorescence background. The fluorescence may stem from the molecules under investigation or from other molecules in the sample. The latter situation may often arise when measuring on food samples, where the sample preparation is absent or kept at a minimum. The weakness of the Raman signal may be improved in different ways. (1): by increasing the photon energy of the laser (i.e. by choosing a laser with shorter wavelength) so that it corresponds to a resonance region of the molecule, (2): by improving the signal to noise ratio

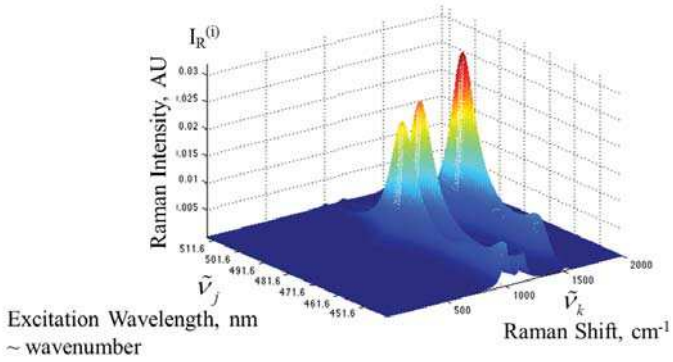

Fig. 4. RADIS, Raman spectra measured with a few different excitation wavelengths close to the electronic resonance of the chromophore.

through the application of a sensitive and cooled CCD detector and (3): by the application of advanced signal processing and multivariate methods. Although, a resonance enhancement of the Raman signal can be achieved by increasing the photon energy of the laser, the amount of absorption is also increased, which may lead to photoinduced degradation of the sample. Since in general the amount of fluorescence increases with shorter wavelength, the resonance enhanced Raman signal may still be partly hidden in the fluorescence background.

On the other hand, when the sample is exposed to a laser with longer wavelength the fluorescence decreases, but unfortunately, this also leads to a lower Raman intensity through the $\tilde{\nu}_{Raman}^4$ dependence shown in Eq.(1). Even though the choice of a longer laser wavelength may result in an acceptable Raman signal, it would be advantageous to enhance the Raman signal and in particular relative to the fluorescence.

This may be achieved in Surface Enhanced Raman Spectroscopy (SERS). The enhancement of the Raman signal may occur, when the scattering molecules are either physisorbed or chemisorbed to a nanostructured metallic surface often made of gold (Au) or silver (Ag). Although a large enhancement can be achieved (up to 10^{14} has been reported), the introduction of a nanostructured surface will in general influence the Raman signal from the native molecules and make the scattering process more complex, so that the interpretation and implementation of SERS require a detailed analysis of the system under investigation.

When a bare nanostructured metal surface is illuminated by the laser, the laser photons interact with the electrons in the surface layer. When the metal and the adsorbed molecules are exposed to laser radiation the incoming laser photons interact with the combined system with the overall result that the intensity of the Raman scattered light is enhanced relative to the intensity of the Raman signal of the free molecules and relative to the fluorescence. The interaction between the incoming light, the metal and the adsorbed molecules depends in a complicated way on the surface morphology, the kind of metal and on the molecule in question. A detailed discussion of the theory and the various implications of SERS can be found in the literature Jernshøj & Hassing (2010); K. Kneipp & (Eds.); Ru & Etchegoin (2009); Willets & Duyne (n.d.). Below, only a brief discussion of SERS is given. Figure 5 illustrates Raman scattering of molecules adsorbed to a nano-structured metal surface.

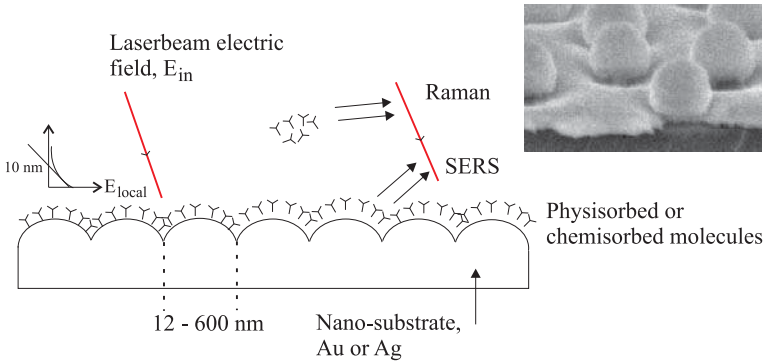

Fig. 5. A simplified schematic representation of SERS. The insert is obtained from R. L. Eriksen and O. Albrektsen (Faculty of Engineering, Institute of Technology and Innovation, University of Southern Denmark). Similar structures can be found in reference R. L. Eriksen & Albrektsen (2010).

A focused laser beam illuminates the molecules adsorbed to the Au or Ag surface. The diameter of the laser beam is typically 0.6 μm and the size of the nano-structure is 12 - 600 nm. The insert shows a SEM-micrograph of a real nano-substrate based on a Si-substrate with 100 nm spheres coated with a 40 nm thick layer of Au. Due to the interaction between the laser light and the electrons in the metal surface a local electric field E_{local} is created outside the metal and very close to the surface. Depending on the specific surface structure E_{local} may be much larger than the incoming electric field, E_{in}, associated with the photons in the laser beam and E_{local} may be rather different in different points on the surface. Surface points, where E_{local} is very high, are called hot-spots. As indicated E_{local} will decrease exponentially with the distance from the surface and only those molecules that are within approximately 10 nm will be influenced significantly by this field. According to electromagnetic theory, the intensity of a light wave is proportional to the absolute square of the electric field associated with the wave. As indicated in the figure, the incoming laser light gives rise to ordinary Raman scattering by the molecules, which are not close to the surface. The Raman intensity of these molecules is proportional to $\mid E_{in} \mid^2$. The molecules adsorbed at the surface interact with the local field and with the electrons in the metal. The result is that both the absorption and the emission parts of the Raman process become proportional to $\mid E_{local} \mid^2$, so that the SERS-signal becomes proportional to $\mid E_{local} \mid^4$. The enhancement of the SERS signal is therefore given by the factor $\mid \frac{E_{local}}{E_{in}} \mid^4$.

Thus in cases, where the local field is just $10E_{in}$, the enhancement of the Raman signal becomes equal to 10000. For comparison, the fluorescence signal is only enhanced with the factor $\mid E_{local}/E_{in} \mid^2$. The difference between the enhancement of the Raman signal and the fluorescence may be attributed to the difference in the coherence properties of the two processes.

SERS can be performed by using nano-substrates with an ordered structure of the SERS-active sites. These can be designed and fabricated with specific applications in mind, including functionalization of the surface with a layer of molecules, which bind reversibly to the specific molecules to be investigated. There are a large variety of commercial nano-substrates available on the market. Another possibility is to form metal colloids and mix the samples with the

colloid solution or by coating e.g. a SiO_2 surface with Au aggregates. Colloidal Au has e.g. been used to chemically identify important components in plant material such as green tea leaves, shredded carrots or shredded red cabbage Zeiri (2007). SERS active substrates made of aggregated Au nanoparticles on a SiO_2 substrates have been applied to detect single cells of different bacteria, which are very important in relation to food products, i.e. Escherichia coli and Salmonella typhimurium W. R. Premasiri & Ziegler (2005). Although Au and Ag based substrates or colloids are the most commonly used, other materials have been applied. Thus, the SERS signal from single cells of Escherichia Coli bacteria has been obtained by mixing ZnO nanoparticles with the bacteria cells R. K. Dutta & Pandey (2009).

2.4 Extracting information from "molecular bar codes" by multivariate analysis

Multivariate analysis is in general applied in order to analyze experimental data by the use of mathematical and statistical methods. The application of multivariate analysis to spectroscopic data has indeed become very important for describing small differences between chemical constituents in samples containing bio-molecules. Spectroscopic data are often analyzed by using Principal Component Analysis (PCA), to which a brief introduction will be given in the following, a thorough explanation of this and other multivariate methods can be found in reference A. K. Smilde & Geladi (2004).

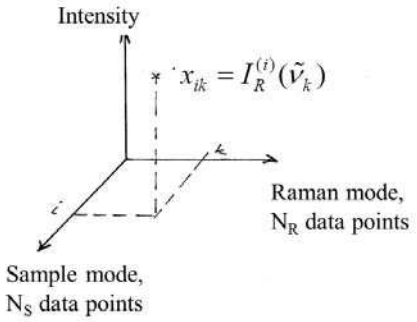

Fig. 6. Raman data matrix: A graphical representation of the data set obtained from N_S Raman experiments, where i is the sample number, $I_{Raman}^{(i)}(\tilde{\nu}_k)$ is the Raman intensity at the k'th energy position in the Raman spectrum.

Assuming that the Raman data from an experiment involving several samples are collected in a matrix denoted $\boldsymbol{X}$, where the matrix element x_{ik} represents the measured Raman intensity for the i'th sample at the energy $\tilde{\nu}_k$ in the Raman spectrum. The number of samples are termed N_S, where $i = 1, 2, ..., N_S$ and each Raman spectrum consists of N_R data points, where $k = 1, 2, ..., N_R$. The data set, containing the Raman intensities for all samples, will then represent a 2-way multivariate data set, which has the dimensions $N_S \times N_R$. A graphical representation of the above is shown in figure 6.

Another way to represent these data is described as follows. The N_R data points define a N_R dimensional coordinate system, where the axes are defined by the energies $\tilde{\nu}_k$. The Raman spectrum for the i'th sample is then represented by a single point, where the position of the point is determined by the Raman intensities at the different energies of the Raman spectrum. The distribution of the N_S sample points reflects the systematic differences between

the Raman spectra of the individual samples. This means that sample points, which represent samples with similar Raman spectra, will lie close together. In general the dimension N_R of this coordinate system is large and some of these dimensions account for similarities in the Raman spectra, i.e. no Raman signal (noise) or identical features in the spectra.

The overall principle behind PCA is to make a favorable coordinate transformation, which represents the significant intensity variations in the spectra. The transformation is in principle carried out by defining a new rotated coordinate system of dimension N_C, where N_C is the number of principal components and typically it is found that $N_C \ll N_R$. For that, a step-by-step procedure is applied. If we assume that the same spectroscopic structure (not necessarily with the same absolute intensity) is present in the Raman spectra in the majority of the samples, then the distribution of the sample points define an average direction in the N_R coordinate system. The unit vector defining this direction is termed the loading vector $\vec{p}_1$, which is calculated from the data by least squares minimization. The score, t_{i1}, for the i'th sample point, is defined as the coordinate of this point in the direction of the loading vector, $\vec{p}_1$. The first principal component is calculated as the outer product (denoted $\otimes$) between the score and the loading vector, and hence is a matrix. This process is carried out again defining next a second loading and second score vector, the process is repeated until the desired accuracy is obtained. In Eq.(2) is given the mathematical expression for the data matrix Hedegaard & Hassing (2008),

$$x_{ik} = \sum_{c=1}^{N_c} t_{ic} p_{kc} + e_{ik}^{(N_C)} \tag{2}$$

where c is the principal component index and $e_{ik}^{(N_C)}$ are elements in a matrix, termed the residual matrix, $\boldsymbol{E}^{(N_C)}$, which in the ideal case contains only noise.

The information obtained from the PCA may be visualized in different ways. One may plot the loadings $\vec{p}_{kc}$ as a function of the energy index, k, for c = 1,2,3,..., N_C. The plot of the c'th loading is proportional to the average Raman spectrum related to the c'th principal component. If the Raman spectra for the N_S samples are almost identical, the plot of the first loadings will show an average of the common features of the spectra, whereas the manifestation of the differences happens in loadings of higher order. Another possibility is to plot the scores, t_{ic}, as a function of the sample index, i for c = 1,2,3,..., N_C, which illustrates the contribution to each loading from each sample. A third option is the score plot, where two of the N_c scores are plotted against each other. The score plot will show a grouping of the sample points according to how significant each of the two loadings contribute to the multivariate model. Since the goal of chemical classification problems is to find the eventual minor differences between the Raman spectra of the different samples, the two latter type of plots clearly reveal, which of the samples are classified correctly as well as the uncertainty of the classification.

The coherent properties of the Raman process can be utilized to create a 3-way multivariate data set. For each sample, the data matrix is constructed by measuring the RADIS data as depicted in figure 6. The elements of the RADIS data matrix x_{ijk}, where the additional index j defines the photon energy of the laser, are $x_{ijk} = I_R^{(i)}(\tilde{\nu}_j \tilde{\nu}_k)$. The 2-way PCA model, which was discussed above, may be generalized into a 3-way model, called Tucker 3 A. K. Smilde & Geladi (2004). A discussion of the mathematical details of applying Tucker 3 on various kind of spectroscopic data can be found in A. K. Smilde & Geladi (2004). Tucker 3 has proven most useful, when compared to other 3-way models, for treating Raman based data A. K. Smilde

& Geladi (2004); Hedegaard & Hassing (2008), which is caused by the high quality of the "molecular bar codes" produced in both dimensions of the RADIS data matrix. In the Tucker 3 model, the elements of the data matrix can be expressed as:

$$x_{ijk} = \sum_{a=1}^{N_A} \sum_{b=1}^{N_B} \sum_{c=1}^{N_c} a_{ia} b_{jb} c_{kc} g_{abc} + e_{ijk}^{(N_A N_B N_C)} \tag{3}$$

where $e_{ijk}^{(N_A N_B N_C)}$ are elements in the residual matrix, a_{ia} are elements in the score vector, b_{jb}, c_{kc} are elements in the loading vectors corresponding to the two dimensions defined by the excitation energy and the Raman shift, and g_{abc} are elements in a matrix reflecting the interactions between the various scores and loadings. One "Tucker 3 component", $\vec{a}_a \otimes \vec{b}_b \otimes \vec{c}_c \cdot g_{abc}$, is analogue to one principal component in PCA, $\vec{t}_c \otimes \vec{p}_c$.

In the 2-way PCA model, described by equation 2, the scores and loadings are determined in the 2 dimensions so that the data is represented by fewest possible parameters. In the 3-way case, the goal is basically the same, but now it is necessary to decompose the three dimensions simultaneously. It is therefore necessary to calculate two loading vectors describing both the Raman and the RADIS spectra for each score vector along the sample dimension of the data. A Tucker 3 model will be applied in subsection 3.2 in the discrimination between molecularly almost identical constituents, α- and β-carotene, when the amount of one of the constituent is very small compared to the other.

3. Three real life applications of Raman spectroscopy and multivariate analysis

The applicability of Raman spectroscopy in food analysis is demonstrated through the discussion of three real life applications, namely 1.) Revelation of a content of minced pork in minced lamb by applying Raman imaging and multivariate analysis, 2.) Discrimination between two anti-oxidants in a mixture by applying RADIS and three-way multivariate analysis and 3.) Non-destructive detection of chlorinated pesticide residues on fruits and vegetables applying a portable Raman spectrometer and SERS.

3.1 Raman imaging and multivariate analysis in the revelation of a content of pork in minced lamb

In the first application, it is demonstrated that Raman spectroscopy can be applied to identify a content of pork in minced lamb products available in e.g. supermarkets. The vision is to develop a scanning system operated by the consumer, which automatically, fast and non-destructively controls for a specific content, e.g. pork and reports the outcome to the consumer. A minced lamb product constitutes an inhomogeneous sample, which consists of areas of meat and fat. The scanning system should be based on a combination of Raman measurements and a multivariate analysis, where the laser excitation wavelength has been chosen in accordance with the transmission spectrum of the film covering the minced meat tub. The discussion of the application is divided into two parts, part 1. Methodology and part 2. Implementation. In part 1, the molecular marker(s) in the Raman spectra must be identified, which enables a distinction between meat and fat. The first part is initiated by using the Raman imaging system (532 and 632,8 nm excitation) shown in figure 2a to create a reference Raman data set of isolated fat and meat from pork and lamb. The XY scanning facility of the Raman imaging system is used in order to automatically create a statistically

large reference data set. Measurements have been carried out changing the wavelength and varying the laser power in order to judge, which parameters gave the measurements best suited for identifying the markers and the multivariate analysis. Since the focal distance is changed during the measurements a software has been developed in order to maximize the Raman data by selecting the acceptable Raman spectra from the raw data. The change of focal distance has to be considered in a practical implementation of the method. The different measurements have besides been optimized with respect to a correction for the background signal and normalization. It is found that the spectral region, containing the most information useable in the identification of molecular markers, is from 500 to 1700 cm^{-1}. One conclusion to be drawn from the above measurements is that the wavelength 632,8 nm is more suitable for further measurements, since the laser wavelength 532 nm is placed in a region of larger absorption and hence may lead to sample degradation.

Figure 7 shows averaged reference Raman spectra of freshly slaughtered pork and lamb (meat and fat) obtained with the Raman imaging system, 632,8 nm excitation and the laser power 11 mW on the sample. The numbers given in the brackets are the total numbers of spectra, which are acquired on different places of a given sample.

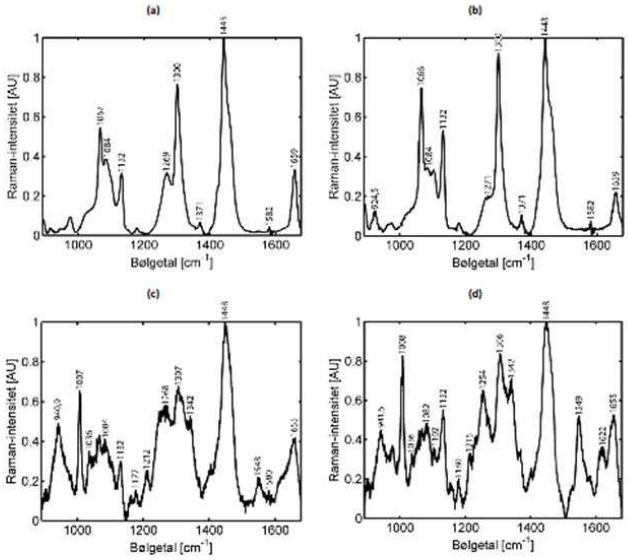

Average spectra : (a) pork-fat, (b) lamb-fat, (c) pork-meat , (d) lamb-meat

Fig. 7. Averaged reference Raman spectra (632,8 nm excitation) from (a.) pork fat (283 spectra), (b.) lamb fat (1493 spectra), (c.) pork meat (48 spectra) and (d.) lamb meat (239 spectra).

The method has been validated by measuring the Raman spectra from samples containing 100% minced pork (meat and fat) and 100% minced lamb (meat and fat). The relative amount of fat in these samples was not specified, but it was less than 20 percent. The number of spectra acquired for minced pork is 366 and for minced lamb 1320. The multivariate method

is based on a Partial Least Squares - Discriminant Analysis (PLS-DA) A. K. Smilde & Geladi (2004), which, contrary to PCA, is a supervised method, where the data is classified according to predefined classes, in the present case the four classes: 100% meat and fat from pork and 100% meat and fat from lamb. The application of the PLS-DA is combined with an algorithm, which is illustrated by the flowchart in figure 8. The results of the validation are shown in table 1.

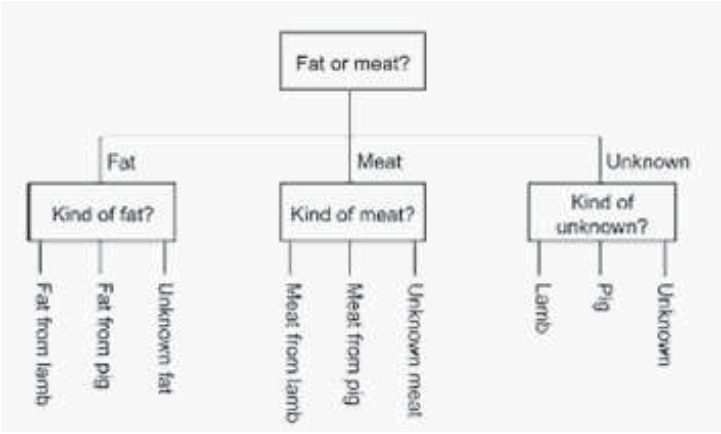

Fig. 8. A flowchart illustrating the different steps of the PLS-DA analysis.

Table 1 should be read as follows: The first row in the table corresponds to the first question in the flowchart and the columns correspond to the questions posed secondly in the flowchart. It follows from the table that the recognition ratio for 1. fat from lamb is 98.0 %, 2. meat from lamb is 20 %, 3. fat from pork is 89.0 % and 4. meat from pork 0 %. Notice that no sample from either lamb or pork has been classified wrongly, i.e. interchanged. The following percentages of the samples have been classified as unknown: fat from lamb fat 2.0 %, meat from lamb 80 %, fat from pork 11.0 % and meat from pork 100 %. It follows from the results that the discrimination between minced pork and lamb can be based on the Raman spectra of fat alone.

		Predicted Content				
Sample	*Content*	*Type*	*Quantity*	*Fat*	*Meat*	*Unknown*
1		Lamb	1257	724	10	523
	100% Minced Lamb	Pig	0	0	0	0
		Unknown	63	15	40	0
2		Lamb	0	0	0	0
	100% Minced Pig	Pig	313	299	0	14
		Unknown	53	37	13	3

Table 1. In the table are listed the results from a programmed algorithm for discrimination between minced lamb (1320 spectra) and pork (366 spectra). The Raman spectra from different points on the two kind of samples are obtained by an automatized XY scanning and 632.8 nm excitation (11 mW) using the Raman imaging system shown in figure 2a.

Further information about the experiments and multivariate analysis can be obtained from the authors (sh@iti.sdu.dk).

2. Implementation. A practical system based on a commercial, portable Raman instrument using 785 nm is under development. The implementation requires that one must consider the following: a.) localization of the areas of fat by using a machine vision system, b.) automatized scanning in order to obtain Raman spectra from fat, c.) automatic adjustment of focus d.) optimization of the excitation volume and laser power, e.) optimization of the statistics (the scanning area, the relative fat content in minced lamb and pork, respectively and the determination of the lower limit with respect to revealing a content of pork in a minced lamb product).

A further development will include the examination of other types of meat than pork and lamb, investigation of samples subjected to different pre-treatments such as freezing or storing inside or outside of a refrigerator. Research on these matters are in progress by the authors of the present paper and in reference Herrero (n.d.). The monitoring of meat quality with respect to molecular composition as a result of decomposition over time (ageing) applying a non-invasive and mobile system based on Raman spectroscopy and fluorescence has been performed in reference G. Jordan (n.d.). Besides, a micro-system including micro-optics and a compact external laser diode cavity with emission wavelength 671 nm suitable for Raman spectroscopy has been developed. The overall dimensions of the micro-system light source is $13 \times 4 \times 1$ mm^3.

3.2 Discrimination between two nearly identical anti-oxidants by applying RADIS and a Tucker 3 multivariate model

Carotenoids are a large family of pigments divided into two main groups carotene and xanthophyll, over 600 different pigments exist. Many of the carotenoid pigments are ubiquitous in nature and has attracted great interest in health and food science due to their nutritional importance Coultate (2002); H. D. Belitz & Schieberle (2004); K. Davies (2004). This importance also most importantly covers the composition of carotenoids in food products rather than specific individual pigments, this topic is subject to an ongoing discussion. This highlights the importance of being able to distinguish between very closely related molecular species, such as lutein, α- and β-carotene.

The second application is a chemical classification problem, in which one must discriminate between pure β-carotene and a mixture of α- and β-carotene. The challenge is that α- and β-carotene have nearly identical Raman spectra.

In reference H. Schulz & Baranski (2005), NIR-FT Raman spectroscopy has been applied in-situ in the analysis of intact plant material, in which the carotenoids are present in their natural concentrations. The carotenoids are present in a large variety of vegetables and fruits: orange, carrot roots, red tomato fruits, green French bean pods, broccoli inflorescence, orange pumpkin, corn and red pepper as well as nectarine, apricot, and watermelon. The spatial distribution of some carotenoids has been obtained by 2D Raman imaging. Although, the Raman spectra and images were recorded with a research, laboratory instrument (with 1064 nm excitation and spectral resolution 4 cm^{-1}), the same measurements could probably also be obtained with one of the recently commercially available portable FT-IR instruments combined with XY translational stage. The analysis performed in reference H. Schulz & Baranski (2005) is based on the three most intense Raman bands of the carotenoids around

1500 (ν_1 band), 1150 (ν_2 band) and 1000 (ν_3 band) cm^{-1}, also shown in figure 1. These bands are characteristic for all carotenoids, but depending on the specific carotenoid molecule, small vibrational shifts of the mentioned bands will be observed. The Raman spectra of the pure carotenoid standards, β-carotene, α-carotene and lutein can be found in figure 3 in reference H. Schulz & Baranski (2005).

In the analysis performed in H. Schulz & Baranski (2005) regarding anti-oxidants in tomatoes, the presence of the 1510 cm^{-1} Raman band has been interpreted as lycopen. A closer examination of the 1510 cm^{-1} band shows a small a-symmetry, which may indicate that β-carotene, where ν_1 = 1515 cm^{-1}, is also present but in a smaller concentration. Additional studies verify this interpretation. If the molecular species that contribute to the spectra are more similar than β-carotene and lycopen, the shifts of the corresponding Raman bands would be smaller and comparable to or less than the resolution of a portable spectrometer. Furthermore, if the difference in carotenoid concentrations is larger, it may be difficult or even impossible to solve a classification problem based exclusively on the vibrational shifts. The spectral distribution in the visible absorption spectra of most carotenoids are rather similar, however small variations in their color are observed. The change in color reflects small differences of the energy of the excited electronic states.

In the following we demonstrate how a small shift in electronic absorption energy can be utilized in a multivariate analysis of the vibrational Raman data. We consider a classification problem, in which the goal is to discriminate between samples with pure β-carotene and samples with a mixture of α- and β-carotene, where the concentration of α-carotene is very small compared to the concentration of β-carotene. From the Raman spectra of the carotenoid standards, it follows that α- and β-carotene have nearly identical Raman spectra: 1515 cm^{-1} (1521), 1156 cm^{-1} (1157) and 1007 cm^{-1} (1006), where the numbers in the brackets correspond to α-carotene.

The classification is performed by applying a Tucker 3 multivariate analysis to the RADIS data matrix obtained with the laser wavelengths 476.5, 488 and 497 nm. When comparing the laser wavelengths with the maxima of the absorption spectra of α- and β-carotene in references (n.d.a); H. D. Belitz & Schieberle (2004); Miller (1934), it is seen that we excite the carotene molecules close to resonance with the lowest electronic transition. The shift in electronic energy can be estimated from the absorption spectra to 268 cm^{-1}. *In the RADIS spectra, this shift will manifest itself as a different resonance enhancement of the Raman signal of the two pigments for each laser wavelength*. The RADIS data matrix will therefore from sample to sample vary along the two dimensions defined by the excitation energy and the Raman shift.

The experimental Raman and RADIS data are obtained from 10 samples, where 5 samples (1 - 5) contain only β-carotene and 5 samples (6 - 10) contain a mixture of 10% α-carotene and 90% β-carotene. The Raman spectra from one sample (476.5 nm excitation) of β-carotene (dashed line) and the mixture of α-carotene and β-carotene (solid line) in solution are shown in figure 9.

The results of a PCA and Tucker 3 analysis of the data are shown in figure 10.

Details about performing the Tucker analysis on similar RADIS data are given in Hedegaard & Hassing (2008). In both the PCA and in the Tucker 3 analysis the classification succeeds and the results are comparable, since the ratios between the average distance between the two classes and the variation within each class are similar. However, further studies involving

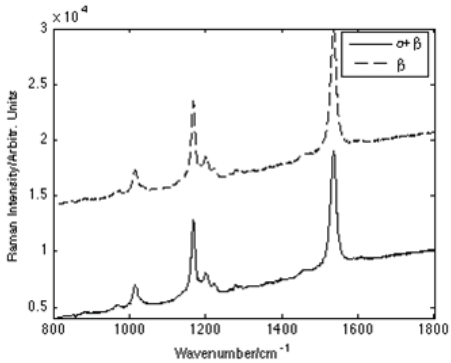

Fig. 9. The Raman spectra from one sample (476.5 nm excitation) of β-carotene (dashed line) and the mixture of α-carotene and β-carotene (solid line) in solution.

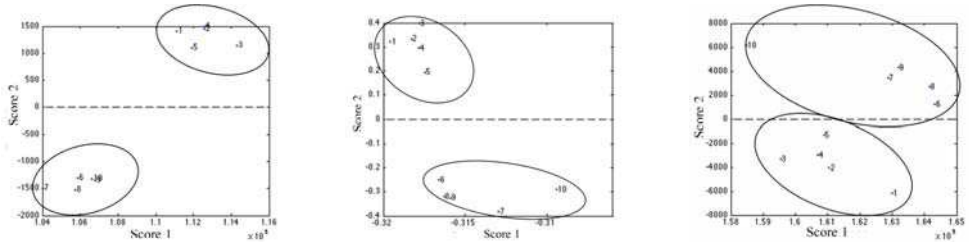

Fig. 10. (a.) Score plot of a 2 component PCA model, excitation wavelength 476 nm (score 2 (t_{i2}) is plotted against score 1 (t_{i1}) for $i = 1, 2....10$), (b.) Score plot of a 4 component Tucker 3 model, 476.5 and 496.5 nm (score 2 (a_{i2}) is plotted against score 1 (a_{i1})) and (c.) Score plot of a 2 component PCA model, 496.5 nm.

10 samples (1 - 10) with only β-carotene and 10 samples (11 - 20) with a mixture of only 0.5% α-carotene and 99.5% β-carotene show that the PCA in most cases leads to a wrong classification, whereas the Tucker 3 model in most cases still leads to a correct classification.

The robustness of the PCA and Tucker 3 models with respect to experimental uncertainties, such as fluctuations in the laser intensity, is different. This is demonstrated in the results shown in figure 11.

The number of samples and the concentration ratio are the same as in figure 10. In general one would expect the classification based on a Tucker 3 analysis to improve by incorporating an extra wavelength. However, by comparing figure 11b with 10b, it is seen that the classification succeeds, but the spread within the classes has increased. The result of the PCA analysis in 11a shows that the PCA classification fails, since it leads to a false grouping of the samples. A closer study of the experimental conditions reveals that the laser intensity at 488 nm fluctuates, which is the explanation for the above results.

In many cases the PCA or PLS-DA analysis of Raman data works fine due to the well resolved spectra. However, it is, as demonstrated above, possible to improve the analysis by including a shift in electronic absorption energy. Another possibility is to include the polarization properties of the Raman spectra in the analysis S. Hassing (2011).

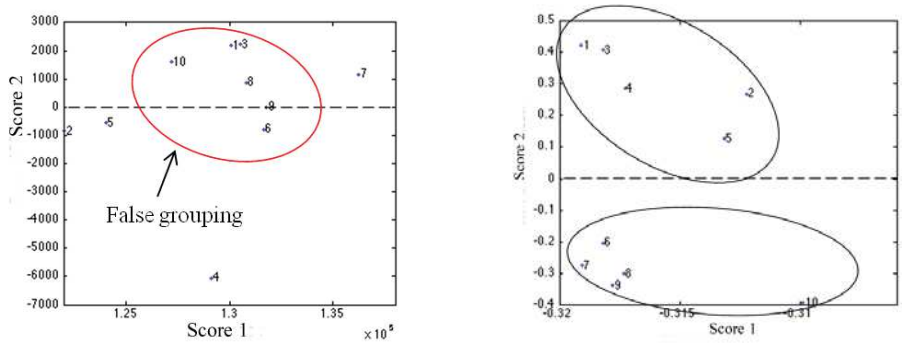

Fig. 11. (a.) Score plot of a 2 component PCA model, excitation wavelength 488 nm (score 2 (t_{i2}) is plotted against score 1 (t_{i1}) for $i = 1, 2....10$), (b.) Score plot of a 4 component Tucker 3 model, 476.5, 488 and 496.5 nm (score 2 (a_{i2}) is plotted against score 1 (a_{i1}) for $i = 1, 2....10$).

3.3 Non-destructive detection of chlorinated pesticide residues on fruits and vegetables applying a portable Raman spectrometer and SERS

We are today facing an increasing exposure to a cocktail of pesticides and other chemicals. The daily exposure to these chemicals, often used in horticulture, agriculture etc., is suspected to cause issues in human health, these include several diseases, reduced fertility and birth defects. One contribution to this exposure is the daily intake of pesticides through food consumption. Besides, an increasing concern with respect to the "cocktail effect", arising when digesting food products containing several pesticides, is seen, since the joint action is not fully understood Danish Ministry of the Environment (2005). Today, more than 800 different pesticides are available and a large number of those are applied to food products Danish Environmental Protection Agency (2005); Veterinary et al. (2003; 2005). Gas Chromatography (GC-multi method, FP017) has been the method of choice for such determination, this procedure, however, is both labor intensive, destructive and non-portable Veterinary & Administration (2003). A calculated intake of pesticides is found by multiplying the average consumption of a commodity with the content of the pesticide and a Hazardous Quotient (HQ) is found by dividing the above mentioned intake with the Acceptable Daily Intake (ADI). The most frequently found pesticides were not including those contributing the most to the hazard quotient, but e.g. dicofol.

It should be noticed that although dicofol is toxic, building up sediments in plants and animals and therefore banned in e.g. Denmark, it has in a spot check been detected on fruit and vegetables imported to Denmark Veterinary et al. (2003). The detection of the pesticide may be due to either contaminated soil, due to a long decomposition time, or due to legal/illegal use in some countries. The acaricide has commonly been applied to a number of fruits among others oranges, apples, grapefruit, lemon, mandarin, clementine, pears, table grape, exotic fruit and tomatoes Veterinary et al. (2003).

The goal of the third application to be discussed is hence a non-destructive, in-situ revelation of the banned pesticide, the organochlorine acaricide and insecticide dicofol, on tomato, apple and carrot by using a portable Raman spectrometer and SERS. A portable system will enable initial spot checking, e.g. in harbors or supermarkets.

As already mentioned, it is not unproblematic to apply SERS or SE(R)RS, since the molecular species should be in close proximity to a nano-structured metal surface in order to obtain an enhanced Raman signal and since the SERS or SE(R)RS spectra (the "molecular bar code") may be different from the Raman spectra of the free molecule. The Raman spectra can for some pesticides in a solution even with a concentration much higher than the detection limit not even be measured. If more pesticides are anticipated on a commodity, the more molecular information available and the more reliably the detection of even structurally related pesticides should be done. Besides, a quantitative analysis based on SERS/SE(R)RS requires in general special attention. Some of the approaches that can be used to ensure that the pesticide is brought reproducibly close to the surface are 1. the pesticide is attached to the molecular species functionalized to the surface of either the colloid or the substrate or 2. the molecules used to functionalize the surface provides molecular pockets, where the pesticide can be trapped close to the surface L. Guerrini (2008). The functionalization, may complicate the SERS spectra, which could necessitate the application of multivariate analysis to elucidate the SERS response from the molecular species under investigation (molecular bar code blurred due to interference from functionalization molecules).

The SERS spectra of an organochlorine pesticide deposited on an Ag substrate, similar to the one shown in figure 12, are earlier reported without any measures taken to ensure the molecular position close to the surface Alak & Vo-Dinh (n.d.). Applying the pesticide reproducibly to the surface itself is an act of art, especially when the foundation for a reproducible, quantitative measurement is required. This touches upon the question of how well the concentration is known, when the pesticide has been applied to the surface. In reference J. C. S. Costa & Corio (n.d.) the behavior of Au nano rods and Ag nano cubes as high performance SERS sensors has been evaluated for amongst others a chlorinated pesticide in a 10^{-7} M solution. In J. C. S. Costa & Corio (n.d.); L. Guerrini (2008) the SERS spectra were obtained by using research instruments.

In the present study a silver Film Over Nano spheres (AgFON) is used as the surface enhancing substrate and the portable Raman spectrometer (DeltaNu InspectorRaman shown in figure 2) as 'the analyzing unit'. The AgFON and periodic particle array (PPA) substrates fabrication process is shown in figure 12. This latter type of substrate can be fabricated according to the same principles governing the fabrication of AgFON's, the differences are, that the PPA's must be made on a transparent material, i.e. cover glass, and the final step is a lift-off of the nano spheres and the metal covering these, leaving only the triangular shaped deposits on the glass. Details about the fabrication process can be found in references A. Henry & Duyne (n.d.); Willets & Duyne (n.d.).

Conventional Raman spectra from the mentioned commodities were first acquired in order to be able to judge the the possible intervenience from the background spectra, see figure 13.

The normal Raman spectrum of the pure pesticide (figure 14) is initially recorded and compared to the pesticide reference spectrum obtained in reference M. L. Nicholas & Bromund (1976) and the obtained SERS spectra as well. In this way it is possible to detect a pesticide, which was not detected by using conventional Raman spectroscopy and to identify the individual peaks from the pesticide in the SERS spectrum.

Next, in figure 15 are seen a Raman spectrum of a 10^{-3} M pesticide dissolved in methanol and a SERS spectrum of the same solution as well as the spectrum of the bare nanostructured surface. The substrate of the type AgFON is seen in the figure as well.

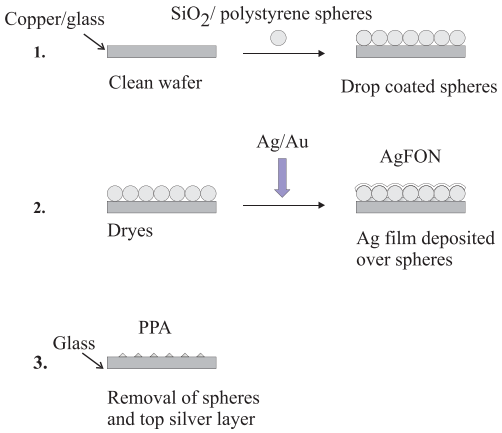

Fig. 12. A schematic representation of the fabrication procedure, when making AgFON's or PPA's using thermal vapor deposition (A. Henry & Duyne (n.d.); Willets & Duyne (n.d.)). In the case of the AgFON, the wafer used in the present research has been copper and the wafer used in the PPA is cover glasses. The metal used is Ag and the thickness of the layer 200 nm and the spheres used are polystyrene spheres.

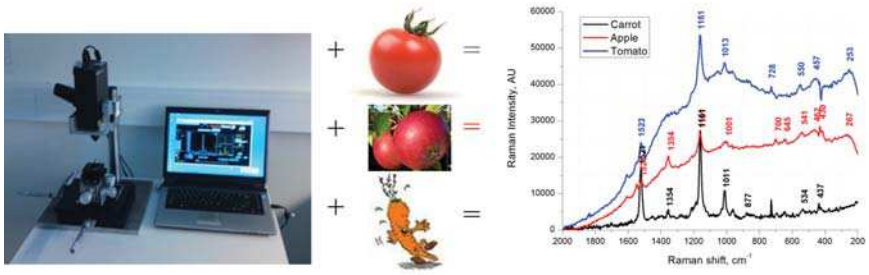

Fig. 13. Conventional Raman spectra of tomato, apple and carrot acquired with Inspector Raman.

The Raman spectrum of the pesticide solution reveals no presence of dicofol only the Raman spectrum of the solvent is observed underlining the need for enhancement. In the SERS spectrum the peak at 1096 cm^{-1} indicates the presence of dicofol, which is seen by comparing the spectrum of dicofol powder with the SERS spectrum. The SERS spectrum contain several Raman bands, but by comparing the spectrum of the bare substrate with the SERS spectrum, it is seen that these overlap with Raman bands found on the bare AgFON. This stresses the need for developing a handling/cleaning procedure or a protective layer for the substrates.

In the implementation of an on-site detection of pesticides on fruits and vegetables, the idea is that the substrate must be transmission based in stead of reflection based as used presently. This will possibly enable a closer contact with the fruit or vegetable surface and a penetration of the laser through the PPA to the commodity, the scattered Raman signal should be detected through the thin glass surface as well. Since dicofol, does not form covalent bonds with the surface, but interacts via other more weak forces, it is difficult to obtain

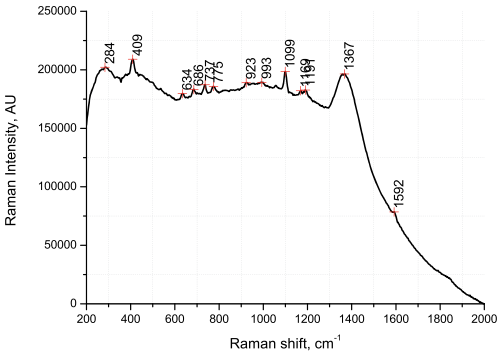

Fig. 14. A Raman spectrum of a pure dicofol powder, which was acquired with Inspector Raman. Notice the peak at 1099 cm^{-1}.

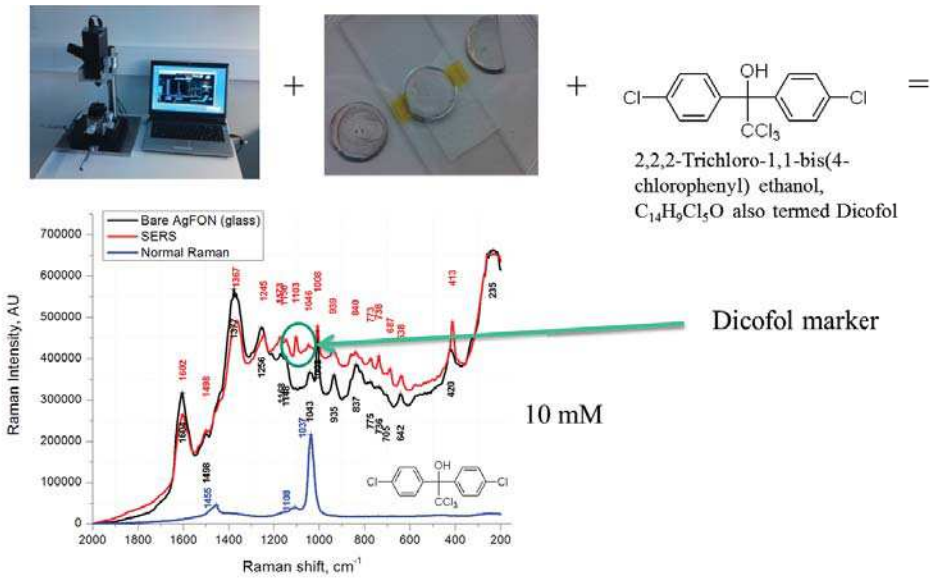

Fig. 15. Raman spectrum of a 10^{-3} M pesticide solution (blue), the SERS spectrum of the same solution (red) and a Raman spectrum of the bare AgFON. The solvent is methanol.

reliable and quantitative measurements without any measures taken to ensure a reproducible binding to the surface. A functionalization with albumin, exploiting the high lipid affinity of organochlorine pesticides, and/or albumin affinity, may be the answer to this problem M. Gülden & Seibert (2002); Maliwal & Guthrie (1981); Moss & Hathway (1964). Besides, a complete displacement of the surface contamination does not take place, which may cause a large background signal. The toxic nature of the pesticides complicates the optimization process of the SERS measurements on these.

In reference (n.d.b); C. Shende & S. Farquaharson (n.d.) it is demonstrated that single pesticides (phosphor- and nitrogen containing) and a mixture of pesticides can be detected fast (5 minutes) in low concentrations (50 - 100 ppm). The SERS setup included a portable FT-Raman spectrometer (785 nm) and specially prepared SERS active capillary probes for chemical extraction of the pesticides and generation of the SERS signal.

Further information about the experiments and fabrication of the substrates as well the possibilities for implementation can be obtained from the authors (kidje@bmb.sdu.dk).

4. Outlook

Raman spectroscopy has through many years been recognized as an advanced research tool for obtaining detailed molecular information. Depending on how the experiments are preformed different kind of information can be revealed such as molecular structure, dynamics and functions of bio-molecules . All due to the coherent nature of the Raman scattering process. Raman spectroscopy meets almost all the requirements listed in the introduction and has, due to the development of highly sensitive CCD-detectors, a variety of small laser sources, hand held spectrometers (dispersive and FT-instruments)and fast computers for the implementation of advanced data processing, the potential for being a fast, non-destructive and molecule specific tool for inspection of food quality. Despite this, Raman spectroscopy has not yet become a standard method within control of food quality, especially not as a standard on-site inspection technique. Our aim has not been to write an exhaustive review article about application of Raman scattering in food analysis Li-Chan (1996), but merely to present an adequate and pinpointed amount of theory and experimental aspects through which an increased understanding enables a more inspiring, creative and intelligent access to applying some kind of Raman spectroscopy within food applications. One major challenge is still to transform the Raman technique from research and analytical laboratories into real life applications, especially the detection of trace amounts of unknown, unwanted substances may be a challenge. We have demonstrated, through the discussion of three rather different case studies, that it is possible, but it requires additional developing work to be performed. Before one attempts to meet the practical challenges, it is therefore mandatory to understand the practical hurdles to be overcome in order to benefit from the high molecular selectivity that Raman spectroscopy can offer. Although there are remaining problems to be solved, we believe that within a few years Raman spectroscopy will develop into the area of analyzing food quality, on-site and non-destructively.

5. References

(n.d.a).

(n.d.b).

A. Henry, J. M. Bingham, E. R. L. D. M. G. C. S. & Duyne, R. P. V. (n.d.). *J. Phys. Chem. C* .

A. K. Smilde, R. B. & Geladi, P. (2004). *Multi-way Analysis: Applications in the Chemical Sciences*.

Alak, A. M. & Vo-Dinh, T. (n.d.). *Analytica Chimica Acta* .

C. Shende, F. Inscore, A. G. P. M. & S. Farquaharson, Journal = *Nondestructive Sensing for Food Safety, Quality, and Natural Resources, Proc. of SPIE 5587* Number = , P. . . T. . A. V. . .-I. . . M. . . Y. . . (n.d.).

Coultate, T. P. (2002). *food, the chemistry of its components*, number 4.

Danish Environmental Protection Agency, D. M. o. t. E. (2005). Bekæmpelsesmiddelstatistik 2005.

Danish Ministry of the Environment, E. P. A. (2005). Bekæmpelsesmiddelforskning fra miljøstyrelsen, kombinationseffekter af pesticider, 98.

eds. R. J. H. Clarke & Hester, R. H. (n.d.). *Advances in Infrared and Raman Spectroscopy (Vol. 1 - 12) and Advances in Spectroscopy (Vol. 13 and onwards)*, Vol. 1 - 12 and 13 and ongoing.

G. Jordan, R. Thomasius, H. S. J. S. W. O. S. B. S. M. M. H. S.-H. D. K. R. S. F. S. . K. D. L. (n.d.). *Journal für Verbraucherschutz und Lebensmittelsicherheit* .

H. D. Belitz, W. G. & Schieberle, P. (2004). *Food Chemistry*, number 3.

H. Schulz, M. B. & Baranski, R. (2005). Potential of nir-ft-raman spectroscopy in natural carotenoid analysis, *Biopolymers* (No. 77): 212 – 221.

Hedegaard, M. & Hassing, S. (2008). Application of raman dispersion spectroscopy in 3-way multivariate data analysis, *J. Raman Spectrosc.* Vol. 7(No. 39): 478 – 489.

Herrero, A. M. (n.d.). *Food Chemistry* .

J. C. S. Costa, R. A. Ando, A. C. S. L. M. R. P. S. S. M. L. A. T. & Corio, P. (n.d.). *Phys. Chem. Chem. Phys* .

Jernshøj, K. D. & Hassing, S. (2009). Analysis of reflectance and transmittance measurements on absorbing and scattering small samples using a modified integrating sphere setup, *Applied Spectroscopy* 8(63): 879–888.
URL: *http://www.opticsinfobase.org*

Jernshøj, K. D. & Hassing, S. (2010). Survival of molecular information under surfaced enhanced resonance raman (serrs) conditions, *J. Raman Spectrosc.* Vol. 7(No. 41): 727 – 738.

K. D. Jernshøj, S. Hassing, R. S. H. & Krohne-Nielsen, P. (2011). Experimental study on polarized se(r)rs of rhodamine 6g adsorbed on porous al_2o_3 substrates, *J. Chem. Phys.* (in print).

K. Davies, e. (2004). *Plant pigments and their manipulation*, Vol. 14.

K. Kneipp, M. M. & (Eds.), H. K. (2006). *Surface-Enhanced Raman Scattering, Physics and Application*.

Kortüm, G. (1969). *Reflectance Spectroscopy, Principles, Methods, Applications*.

L. Guerrini, A. E. Aliaga, J. C. J. S. G.-J. S. S.-C. M. M. C.-V. J. V. G.-R. (2008). Functionalization of ag nanoparticles with the bis-acridinium lucigenin as a chemical assembler in the detection of persistent organic pollutants by surface-enhanced raman scattering, *Analytica Chimica Acta* 624: 286 – 293.

Li-Chan, E. C. Y. (1996). The applications of raman spectroscopy in food science, *Trends in Food Science and Technology* 7: 361 – 370.

Long, D. A. (1969). *The Raman Effect, A Unified Treatment of the Theory of Raman Scattering by Molecules*.

Long, D. A. (2002). *Raman Spectroscopy*.

M. Gülden, S. Mörchel, S. T. & Seibert, H. (2002). Impact of protein binding on the availability and cytotoxic potency of organochlorine pesticides and chlorophenols in vitro, *Toxicology* 175: 201 – 213.

M. L. Nicholas, D. L. Powell, T. R. W. & Bromund, R. H. (1976). Reference raman spectra of ddt and five structurally related pesticides containing the norbornene group, *Journal of the AOAC* 59(1): 197 – 208.

Maliwal, B. P. & Guthrie, F. E. (1981). Interaction of insecticides with human serum albumin, *Molecular Pharmacology* 20: 138–144.

Martin Hedegaard, Christoph Krafft, H. J. D. L. E. J.-S. H. & Popp, J. (2010). Discriminating isogenic cancer cells and identifying altered unsaturated fatty acid content as

associated with metastasis status, using k-means clustering and partial least squares-discriminant analysis of raman maps, *Analytical Chemistry* 82(7): 2797 – 2802.
McCreery, R. L. (2000). *Raman Spectroscopy for Chemical Analysis*.
Miller, E. S. (1934). Quantative absorption spectra of the common carotenoids, *Plant Physiol.* 9(3): 693Ű694.
Mortensen, O. S. (1981). Raman dispersion spectroscopy (radis), 1 - phenomenology, *J. Raman Spectroscopy* 11(5): 321 – 333.
Mortensen, O. S. & Hassing, S. (1980). *Polarization and Interference Phenomena in Resonance Raman Scattering in Advances in Infrared and Raman Spectroscopy, R. J. H. Clark and R. E. Hester (eds.)*, Vol. 6.
Moss, J. A. & Hathway, D. E. (1964). Transport of organic compounds in the mammal, *Biochem. J.* 91: 384.
Plazek, G. (1934). *Rayleigh-Streuung und Raman-Effekt, in Handbuch der Radiologie, E. Marx (ed.)*, Vol. 3048.
R. K. Dutta, P. K. S. & Pandey, A. C. (2009). Surface enhanced raman spectra of escherichia coli cells using zno nanoparticles, *Digest Journal of Nanomaterials and Biostructures* 4(1): 83 – 87.
R. L. Eriksen, A. Pors, J. D. A. C. S. & Albrektsen, O. (2010). Fabrication of large area homogenous metallic nanostructures for optical sensing using colloidal lithography, *Microelectronic Engineering* 87: 333 – 337.
Raman, C. V. & Krishnan, K. S. (1928). A new type of secondary radiation, *Nature* 3048(121): 501.
Ru, E. C. L. & Etchegoin, P. G. (2009). *Principles of Surface-Enhanced Raman Spectroscopy and related plasmonic effects*.
S. Hassing, K. D. Jernshøj, M. H. (2011). Solving chemical classification problems using polarized raman data, *J. Raman Spectrosc.* 42(1): 21 – 35.
URL: *onlinelibrary.wiley.com/doi/10.1002/jrs.2666/pdf/*
Smith, E. & Dent, G. (2005). *Modern Raman Spectroscopy, A Practical Approach*.
Veterinary, D. & Administration, F. (2003). Pesticidrester i foedevarer, bilag 2, analysemetoder anvendt i undersøgelser 2003.
Veterinary, D., Food Administration, M. o. F. & Affairs, C. (2003). Pesticides, food monitoring, 1998-2003, part 2.
Veterinary, D., Food Administration, M. o. F. & Affairs, C. (2005). Pesticidrester i fødevarer **2005** - resultater fra den danske pesticidkontrol.
Vidi, S. (2003). *Fourier-transform spectroscopy instrumentation engineering*.
W. R. Premasiri, D. T. Moir, M. S. K. N. K. G. J. & Ziegler, L. D. (2005). Characterization of the surface enhanced raman scattering (sers) of bacteria, *J. Phys. Chem. B* 109: 321 – 320.
Willets, K. A. & Duyne, R. P. V. (n.d.). *Ann. Rev. Phys. Chem.* .
Zeiri, L. (2007). Sers of plant material, *J. Raman Spectrosc.* 38: 950 – 955.

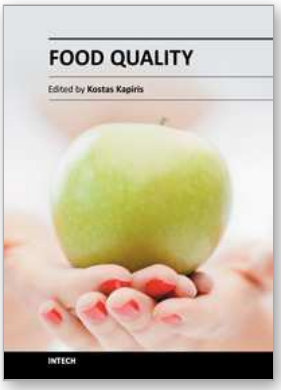

Food Quality

Edited by Dr. Kostas Kapiris

ISBN 978-953-51-0560-2
Hard cover, 134 pages
Publisher InTech
Published online 20, April, 2012
Published in print edition April, 2012

The book discusses the novel scientific approaches for the improvement of the food quality and offers food scientists valuable assistance for the future. The detailed methodologies and their practical applications could serve as a fundamental reference work for the industry and a requisite guide for the research worker, food scientist and food analyst. It will serve as a valuable tool for the analysts improving their knowledge with new scientific data for quality evaluation. Two case study chapters provide data on the improvement of food quality in marine and land organisms in the natural environment.

How to reference

In order to correctly reference this scholarly work, feel free to copy and paste the following:

S. Hassing, K.D. Jernshøj and L.S. Christensen (2012). Raman Spectroscopy: A Non-Destructive and On-Site Tool for Control of Food Quality?, Food Quality, Dr. Kostas Kapiris (Ed.), ISBN: 978-953-51-0560-2, InTech, Available from: http://www.intechopen.com/books/food-quality/raman-spectroscopy-a-non-destructive-and-on-site-tool-for-control-of-food-quality

INTECH
open science | open minds

InTech Europe
University Campus STeP Ri
Slavka Krautzeka 83/A
51000 Rijeka, Croatia
Phone: +385 (51) 770 447
Fax: +385 (51) 686 166
www.intechopen.com

InTech China
Unit 405, Office Block, Hotel Equatorial Shanghai
No.65, Yan An Road (West), Shanghai, 200040, China
中国上海市延安西路65号上海国际贵都大饭店办公楼405单元
Phone: +86-21-62489820
Fax: +86-21-62489821